Merging Photoredox Catalysis with Organocatalysis: The Direct Asymmetric Alkylation of Aldehydes

David A. Nicewicz, *et al.*

Science **322**, 77 (2008);
DOI: 10.1126/science.1161976

Science (print ISSN 0036-8075; online ISSN 1095-9203) is published weekly, except the last week in December, by the American Association for the Advancement of Science, 1200 New York Avenue NW, Washington, DC 20005.

8. C. Resini, T. Montanari, G. Busca, J.-M. Jehng, I. E. Wachs, *Catal. Today* **99**, 105 (2005).
9. T. G. Alkhazov, E. A. Ismailov, A. Yu, A. I. Kozharov, *Kinet. Katal.* **19**, 611 (1978).
10. M. S. Kane, L. C. Kao, R. K. Mariwala, D. F. Hilscher, H. C. Foley, *Ind. Eng. Chem. Res.* **35**, 3319 (1996).
11. M. F. R. Pereira, J. J. M. Órfão, J. L. Figueiredo, *Appl. Catal. A* **218**, 307 (2001).
12. J. Zhang *et al.*, *Angew. Chem. Int. Ed.* **46**, 7319 (2007).
13. G. Mestl, N. I. Maksimova, N. Keller, V. V. Roddatis, R. Schlögl, *Angew. Chem. Int. Ed.* **40**, 2066 (2001).
14. See supporting material on *Science* Online.
15. J.-H. Zhou *et al.*, *Carbon* **9**, 1379 (2007).
16. K. D. Chen, E. Iglesia, A. T. Bell, *J. Phys. Chem. B* **105**, 646 (2001).
17. M. Salmeron, R. Schlögl, *Surf. Sci. Rep.* **63**, 169 (2008).
18. T. I. T. Okpalugo, P. Papakonstantinou, H. Murphy, J. McLaughlin, N. M. D. Brown, *Carbon* **43**, 153 (2005).
19. L. M. Madeira, M. F. Portela, *Catal. Rev.* **44**, 247 (2002).
20. F. Atamny *et al.*, *Mol. Phys.* **76**, 851 (1992).
21. M. L. Toebes, J. M. P. van Heeswijk, J. H. Bitter, A. J. van Dillen, K. P. de Jong, *Carbon* **42**, 307 (2004).
22. A. M. Puziy, O. I. Poddubnaya, A. M. Ziatdinov, *Appl. Surf. Sci.* **252**, 8036 (2006).
23. S. J. Clark *et al.*, *Z. Kristallogr.* **220**, 567 (2005).
24. J. P. Perdew, K. Burke, M. Ernzerhof, *Phys. Rev. Lett.* **77**, 3865 (1996).

25. We thank the Max Planck Society; U. Wild, A. Klein-Hoffmann, and J. Thielemann for technical assistance; Berliner Elektronenspeicherring-Gesellschaft für Synchrotronstrahlung for support of in situ XPS measurements; and M. A Smith for helpful discussions. Supported by the CANAPE project of the 6th Framework Programme of European Commission and the ENERCHEM project of the Max Planck Society.

Supporting Online Material

www.sciencemag.org/cgi/content/full/322/5898/73/DC1
Materials and Methods
Figs. S1 to S6
Table S1
References

17 June 2008; accepted 21 August 2008
10.1126/science.1161916

Merging Photoredox Catalysis with Organocatalysis: The Direct Asymmetric Alkylation of Aldehydes

David A. Nicewicz and David W. C. MacMillan*

Photoredox catalysis and organocatalysis represent two powerful fields of molecule activation that have found widespread application in the areas of inorganic and organic chemistry, respectively. We merged these two catalysis fields to solve problems in asymmetric chemical synthesis. Specifically, the enantioselective intermolecular α-alkylation of aldehydes has been accomplished using an interwoven activation pathway that combines both the photoredox catalyst $Ru(bpy)_3Cl_2$ (where bpy is 2,2′-bipyridine) and an imidazolidinone organocatalyst. This broadly applicable, yet previously elusive, alkylation reaction is now highly enantioselective and operationally trivial.

Nature's ability to convert solar energy to chemical energy in photosynthesis has inspired the development of a host of photoredox systems in efforts to mimic this process. Arguably the most studied one-electron photoredox catalyst has been $Ru(bpy)_3^{2+}$ (where bpy is 2,2′-bipyridine): an inorganic complex that has facilitated important advances in the areas of energy storage, hydrogen and oxygen evolution from water, and methane production from carbon dioxide (*1*, *2*). Given its proven ability to mediate electron transfer, it is surprising that $Ru(bpy)_3^{2+}$ has not found a substantial application in organic synthesis, wherein a large number of fundamental reactions rely on the generation and exploitation of radicals or single-electron intermediates (*3*).

Over the past decade, the field of organocatalysis has grown at a dramatic pace, providing more than 130 chemical reactions that rapidly facilitate enantioselective C–C, C–O, C–N, and C–halogen bond formation (*4*, *5*). Whereas a broad range of reaction types have recently succumbed to this mode of catalysis (including aldol, Friedel-Crafts, and cycloadditions), it is important to consider that nearly all organocatalytic bond constructions are restricted to two-electron pathways, wherein the highest occupied molecular orbital of an electron-rich substrate reacts with the lowest unoccupied molecular orbital of an electron-deficient partner. Recently, however, our laboratory introduced the concept of organo–singly occupied molecular orbital (SOMO) catalysis, a one-electron mode of activation that has enabled the development of several useful transformations (*6*–*10*).

Given the widespread success of both electron transfer catalysis and organocatalysis, we recently questioned whether it might be possible to merge these two powerful areas, with the goal of solving long-standing, yet elusive problems in chemical synthesis. More specifically, as a blueprint for reaction invention, we hoped to exploit the lessons of photoredox enzymatic catalysis (*11*), wherein a series of consecutive low-barrier, open-shell steps are energetically preferred to high-barrier, two-electron pathways. On this basis, we hypothesized that the enantioselective catalytic α-alkylation of aldehydes (*12*–*15*), a widely sought yet elusive transformation, might be brought to fruition via the marriage of inorganic electron transfer and organic catalysis (Fig. 1).

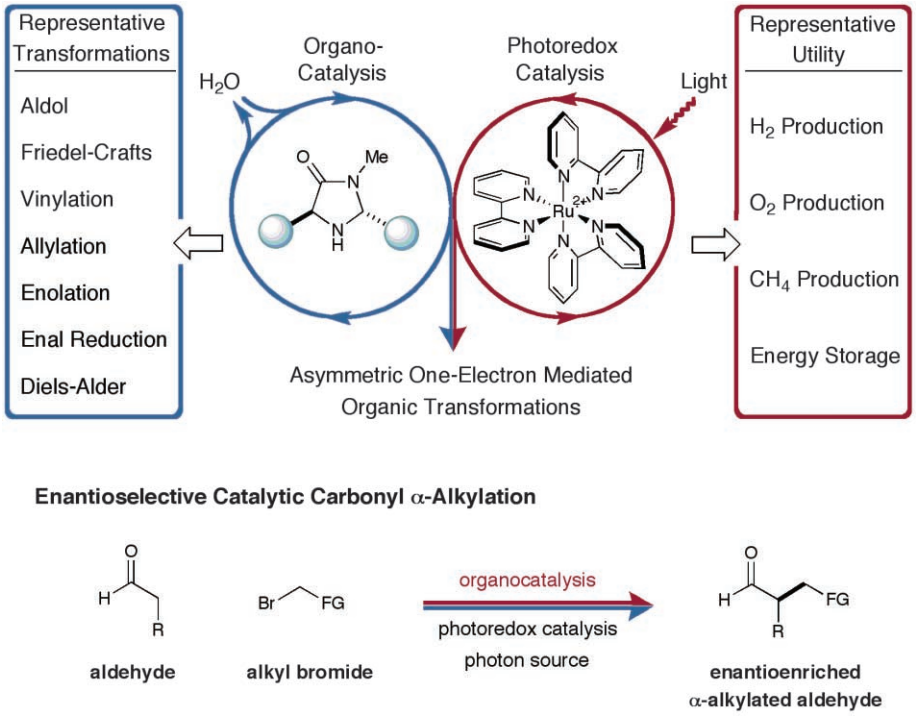

Fig. 1. Merging amine catalysis and organometallic photoredox catalysis to enable asymmetric organic transformations. Me, methyl; R, generic organic substituent; FG, electron-withdrawing functional group.

Contribution from Merck Center for Catalysis, Department of Chemistry, Princeton University, Princeton, NJ 08544, USA.

*To whom correspondence should be addressed. E-mail: dmacmill@princeton.edu

We proposed that two interwoven catalytic cycles might be engineered to simultaneously generate an electron-rich enamine from the condensation of an aldehyde and an amine catalyst and an electron-deficient alkyl radical via reduction of an alkyl bromide with a Ru photoredox catalyst (Fig. 2). Given that electron-deficient radicals are known to rapidly combine with π-rich olefins to forge even the most elusive C–C bonds (*16*, *17*), we hoped that this dual-catalysis mechanism would successfully converge to enable the direct coupling of aldehydes with α-bromo ketones or esters. As a critical design element, we presumed that the use of a suitable chiral amine catalyst would induce high enantioselectivity. Moreover, we recognized that the interaction of a SOMOphilic enamine with an electron-deficient radical is the converse mechanism to our previously described SOMO activation studies. As such, a complementary array of catalytic bond constructions should be possible.

A detailed description of our dual-catalysis aldehyde alkylation is presented in Fig. 2. It has long been established that $Ru(bpy)_3^{2+}$ (**1**) will readily accept a photon from a variety of light sources to populate the $*Ru(bpy)_3^{2+}$ (**2**) metal-to-ligand charge transfer (MLCT) excited state (*1*, *2*). Although $*Ru(bpy)_3^{2+}$ (**2**) can function as a reductant or an oxidant, we postulated that this high-energy intermediate would efficiently remove a single electron from a sacrificial quantity of enamine, to initiate our first catalytic cycle and provide the electron-rich $Ru(bpy)_3^{+}$ (**3**). Given that $Ru(bpy)_3^{+}$ (**3**) has been shown to be a potent reductant [–1.33 V versus saturated calomel electrode (SCE) in CH_3CN] (*18*), we anticipated that single-electron transfer (SET) to the α-bromocarbonyl substrate **4** would rapidly furnish the electron-deficient alkyl radical **5** while returning $Ru(bpy)_3^{2+}$ (**1**) to the catalytic cycle ($E_{1/2}$ for phenacyl bromide = –0.49 V versus SCE in CH_3CN, where $E_{1/2}$ is the half reduction potential) (*19*–*22*). As a central design consideration, we recognized that the redox potentials of $Ru(bpy)_3^{2+}$ can be readily fine-tuned by ligand modification (*1*).

Concurrent with this photoredox pathway, the organocatalytic cycle would begin with condensation of the imidazolidinone catalyst **6** and the aldehyde substrate **7** to form enamine **8**. At this stage, we expected the two catalytic cycles to intersect via the addition of the SOMOphilic enamine **8** to the electron-deficient alkyl radical **5**, thereby achieving the key alkylation step. This coupling event would concomitantly produce an electron-rich α-amino radical **9**, a single-electron species that has a low barrier to oxidation (–0.92 to –1.12 V versus SCE in CH_3CN) (*23*). Once again, convergence of our catalytic cycles should ensure SET from α-amino radical **9** to the $*Ru(bpy)_3^{2+}$ (**2**) excited state to produce the iminium ion **10** and regenerate the active reductant, $Ru(bpy)_3^{+}$ (**3**)—a step that would close the photoredox cycle (*24*). Hydrolysis of the resulting iminium **10** would reconstitute the amine catalyst **6** while delivering the requisite enantioenriched α-alkyl aldehyde product.

From the outset, we understood that the utility of this alkylation reaction would rely on the identification of an amine catalyst that could generically enforce high levels of enantiocontrol in the coupling of the pivotal π-rich enamine with a diverse array of electron-deficient radicals. On the basis of density functional theory (DFT) calculations (*25*, *26*), we proposed that the imidazolidinone catalyst **6** should selectively form an enamine **8** (DFT-**8**), that projects the 2π electron system away from the bulky *tert*-butyl group, whereas the electron-rich olefin will selectively populate an (*E*)-configuration to minimize nonbonding interactions with the imidazolidinone ring (Fig. 2). In terms of enantiofacial discrimination, the calculated DFT-**8** structure also reveals that the methyl group on the catalyst system will effectively shield the *Re* face of the enamine, leaving the *Si* face exposed for enantioselective radical addition. We have found that the trans methyl, *tert*-butyl 2,5-disubstituted imidazolidinone **6** is an excellent enamine catalyst for transformations performed at room temperature. Specifically, catalyst **6** provides excellent levels of kinetic enantiocontrol yet does not readily participate in enamine formation with the 2,2′-disubstituted aldehyde-alkylation adduct, a step that would erode product enantiopurity via epimerization.

This new asymmetric alkylation protocol was first examined using octanal and bromo diethylmalonate as the coupling partners, along with a catalyst combination of $Ru(bpy)_3Cl_2$ (**1**) and imidazolidinone **6**, and a 15-W fluorescent light source (Table 1) (*27*). To our great delight, preliminary studies revealed the successful execution of our dual-cycle design ideals to provide (*R*)-2-malonyloctanal with excellent levels of enantiocontrol and reaction efficiency [entry 1, 93% yield, 90% enantiomeric excess (ee)]. Experiments that probe the scope of the aldehyde component in this new alkylation reaction are summarized in Table 1 (entries 1 to 6). Chemical functionalities that are often prone to either oxidation or reduction (e.g., olefins, esters, carbamates, and arenes) were found to be inert to these mild redox conditions (entries 2 to 5, 66 to 92% yield, 90 to 95% ee). Moreover, the steric demand of the α-formyl substituent has little impact on the efficiency and enantioinduction of the alkylation process (entries 1 and 4, substituent is *n*-hexyl versus cyclohexyl, 83 to 93% yield, 90 to 95% ee), a point that is underscored by the successful use of adamantyl acetaldehyde (entry 6, 63% yield, 93% ee).

A broad array of electron-deficient α-bromo carbonyls can effectively serve as alkylating agents

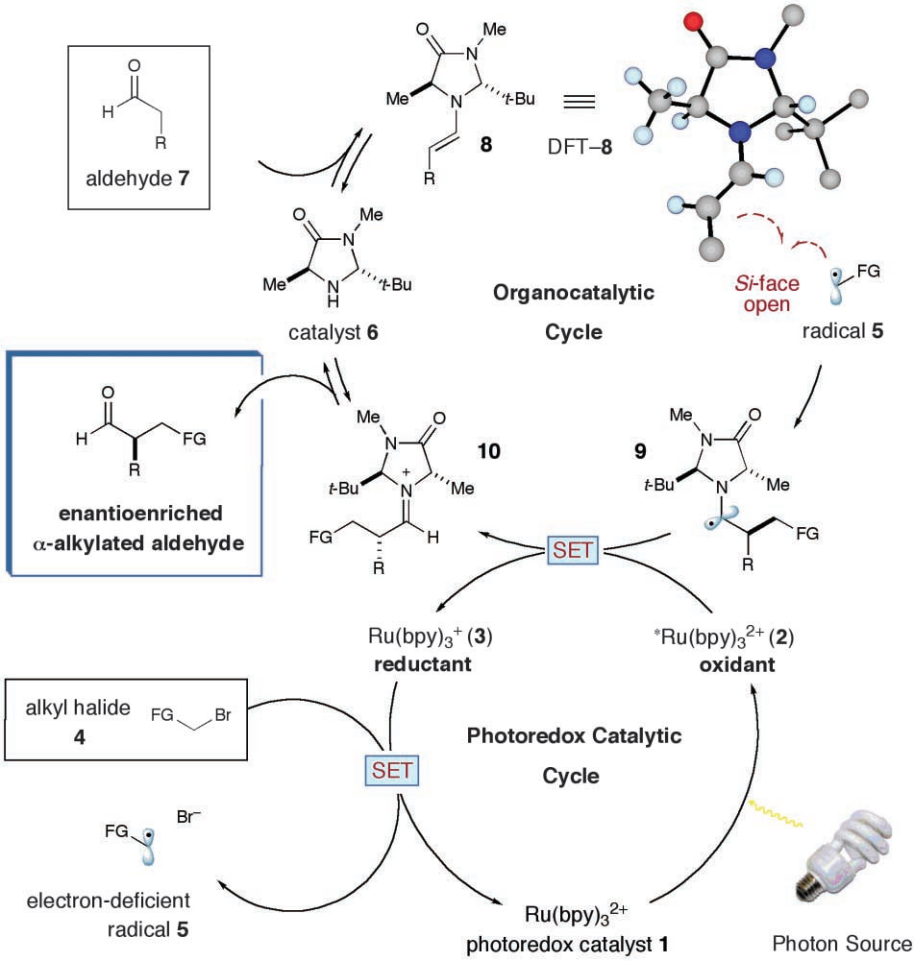

Fig. 2. Merging photoredox catalysis with organocatalysis. Proposed mechanism. *t*-Bu, *tert*-butyl.

Table 1. Survey of the bromide and aldehyde scope in the direct α-alkylation of aldehydes. Y, any organic substituent (alkyl, aryl, alkenyl, alkynyl, etc.); DMF, *N*,*N*′-dimethylformamide; Tf, triflate; Me, methyl; Et, ethyl; Hex, hexyl; Ph, phenyl; *t*-Bu, *tert*-butyl; Boc, *tert*-butyl carbamoyl.

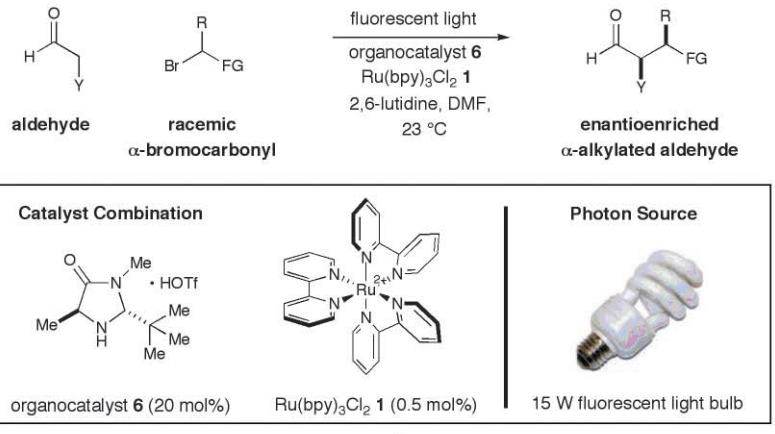

entry	aldehyde	product*
1	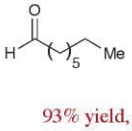	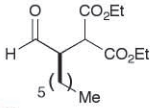 93% yield, 90% ee
2	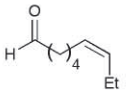	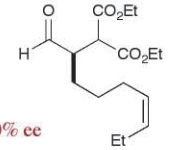 86% yield, 90% ee
3	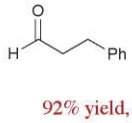	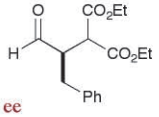 92% yield, 90% ee
4	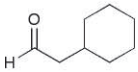	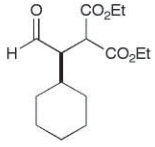 83% yield, 95% ee
5	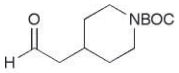	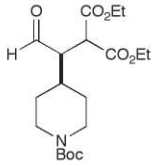 66% yield, 91% ee
6		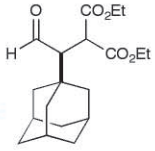 63% yield†, 93% ee

entry	α-bromocarbonyl	product‡
7	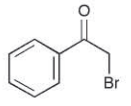	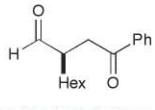 84% yield, 96% ee
8	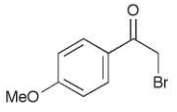	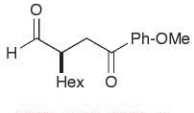 87% yield, 96% ee
9	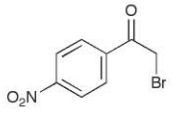	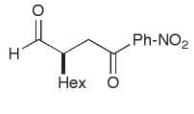 84% yield, 95% ee
10	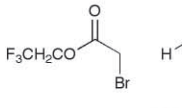	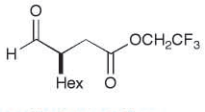 80% yield, 92% ee
11	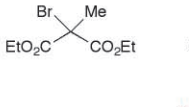	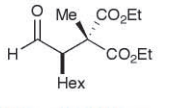 80% yield, 88% ee
12	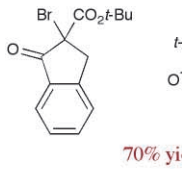	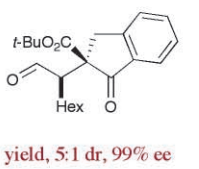 70% yield, 5:1 dr, 99% ee

*Reactions performed with diethyl bromomalonate. †40 mole percent of organocatalyst **6** was employed. ‡Reactions performed with octanal.

in this tandem catalysis manifold (Table 1, entries 7 to 12). For example, bromoacetophenone systems of diverse electronic orientation (*p*-OMe, *p*-NO_2, *p*-H) provide almost identical selectivity and efficiency profiles (entries 7 to 9; 84 to 87% yield, 95 to 96% ee). Whereas α-bromo esters are readily tolerated ($BrCH_2CO_2Et$, 53% yield, 94% ee), we have found that superior yields are obtained with markedly electron-deficient carbonyls such as the trifluoroethyl ester (80% yield, 92% ee). As a testament to the versatility and power of one-electron mediated pathways, we have found that tertiary bromo-substituted alkylating agents can be readily employed to forge all-carbon quaternary centers, (entries 11 and 12, ≥70% yield, 88 to 99% ee). Moreover, racemic α-bromo radical precursors can be employed to generate quaternary stereocenters with appreciable levels of diastereocontrol (entry 12, 5:1 diastereomeric ratio), illustrating the capacity of the pivotal enamine intermediate to differentiate the enantiotopic faces of a trisubstituted carbon-centered radical. The sense of asymmetric induction observed in all cases (Table 1) is consistent with selective addition of the electron-deficient radical to the *Si* face of the enamine **8**, in complete accord with the calculated structure DFT-**8**.

With respect to operational convenience, it is important to consider that this alkylation protocol does not require any heating or cooling, all of the components employed in this study (substrates, catalysts, and solvents) are commercially available and inexpensive, and a simple household 15-W fluorescent light bulb can be employed as a suitable light source. A 2-g alkylation was readily accomplished using the outlined procedure (entry 7).

We have conducted a series of control experiments and luminescence quenching studies to test the validity of our proposed dual-cycle pathway and gain further insight into the photonic requirements for metal-mediated redox catalysis. The control experiments were performed using octanal with α-bromoacetophenone or diethyl bromomalonate in the presence of various catalyst combinations and a 15-W fluorescent light source (unless otherwise stated). Several observations are of note: Rigorous exclusion of light failed to produce even trace quantities of the coupling adduct. Moreover, removal of $Ru(bpy)_3^{2+}$ from our standard protocol resulted in <10% alkylation product over an extended timeframe (24 hours). High levels of reaction efficiency (>80%) can be obtained in the absence of $Ru(bpy)_3^{2+}$ if a high-energy UV irradiation source (300 to 350 nm) is employed in a photobox environment. In this specific case, we assume that a monocyclic catalysis mechanism is operable wherein the α-bromocarbonyl is converted to the requisite electron-deficient radical via photolytic bond homolysis (as opposed to catalytic SET reduction). Execution of our standard reaction with a light source specifically tuned to the $Ru(bpy)_3^{2+}$ MLCT absorption band (465 ± 20 nm full width

at half maximum, 500 mW) resulted in a dramatic acceleration in overall rate (90 min) as compared with the use of a typical household 15-W fluorescent bulb (6 hours), which operates with a wide spectral window (~400 to 700 nm). The use of the same 465-nm photon source in the absence of $Ru(bpy)_3^{2+}$ resulted in only trace product formation (<5%) (*28*). These experiments provide strong evidence of the participation of the $*Ru(bpy)_3^{2+}$ (**2**) excited state in the catalytic cycle.

With respect to our luminescence quenching studies, it has long been established that certain electron-deficient C–Br bonds can quench the emission intensity of $*Ru(bpy)_3^{2+}$ by SET (*29*). However, we did not observe a decrease in $*Ru(bpy)_3^{2+}$ luminescence in the presence of α-bromoacetophenone or diethyl bromomalonate, a result that negates the possibility that $*Ru(bpy)_3^{2+}$ (**2**) is participating as a reductant in our tandem catalysis sequence. In contrast, enamine **8** (pregenerated in stoichiometric quantities) does decrease the $*Ru(bpy)_3^{2+}$ emission intensity with a small but significant Stern-Volmer constant of 10 M^{-1} (see fig. S1) (*30*). These observations collectively support our mechanistic proposal that the $*Ru(bpy)_3^{2+}$ (**2**) excited state behaves as an oxidant in our photoredox cycle.

We have also gained circumstantial evidence that enamine **8** is the organocatalytic intermediate that participates in the key bond-forming step. More specifically, exposure of 2-phenylcyclopropyl acetaldehyde to our standard reaction protocol resulted in clean conversion (83% yield) to the corresponding alkylation product (see supporting online material). Failure of this radical clock substrate to undergo cyclopropyl ring opening clearly indicates that a 3π electron SOMO activated intermediate is not operative in the organocatalytic cycle.

References and Notes

1. K. Kalyanasundaram, *Coord. Chem. Rev.* **46**, 159 (1982).
2. A. Juris *et al.*, *Coord. Chem. Rev.* **84**, 85 (1988).
3. P. Renaud, M. P. Sibi, Eds., *Radicals in Organic Synthesis* (Wiley-VCH, Weinheim, Germany, 2001).
4. A. Berkessel, H. Gröger, Eds., *Asymmetric Organocatalysis: From Biomimetic Concepts to Applications in Asymmetric Synthesis* (Wiley-VCH, Weinheim, Germany, 2005).
5. P. I. Dalko, Ed., *Enantioselective Organocatalysis: Reactions and Experimental Procedures* (Wiley-VCH, Weinheim, Germany, 2007).
6. T. D. Beeson, A. Mastracchio, J. B. Hong, K. Ashton, D. W. C. MacMillan, *Science* **316**, 582 (2007); published online 28 March 2007 (10.1126/science. 1142696).
7. H. Jang, J. B. Hong, D. W. C. MacMillan, *J. Am. Chem. Soc.* **129**, 7004 (2007).
8. H. Kim, D. W. C. MacMillan, *J. Am. Chem. Soc.* **130**, 398 (2008).
9. A SOMO activation mechanism has also been reported for the α-oxidation of aldehydes (*10*).
10. M. Sibi, M. Hasegawa, *J. Am. Chem. Soc.* **129**, 4124 (2007).
11. H. B. Gray, J. R. Winkler, *Annu. Rev. Biochem.* **65**, 537 (1996).
12. An intramolecular α-formyl alkylation has been reported (*13*).
13. N. Vignola, B. List, *J. Am. Chem. Soc.* **126**, 450 (2004).
14. For a catalytic enantioselective alkylation of racemic α-bromoesters, see (*15*).
15. X. Dai, N. A. Strotman, G. C. Fu, *J. Am. Chem. Soc.* **130**, 3302 (2008).
16. P. Renaud, S. Schubert, **1990**, *Synlett* 624 (1990).
17. G. A. Russell, K. Wang, *J. Org. Chem.* **56**, 3475 (1991).
18. C. R. Bock *et al.*, *J. Am. Chem. Soc.* **101**, 4815 (1979).
19. Value was corrected from the $Ag/Ag^+ClO_4^-$ electrode (*20*).
20. D. D. Tanner, H. K. Singh, *J. Org. Chem.* **51**, 5182 (1986).
21. $Ru(bpy)_3^+$ has previously been shown to reduce phenacyl bromide (*22*).
22. S. Fukuzumi, S. Mochizuki, T. Tanaka, *J. Phys. Chem.* **94**, 722 (1990).
23. D. D. M. Wayner, J. J. Dannenberg, D. Griller, *Chem. Phys. Lett.* **131**, 189 (1986).
24. The possibility of direct one-electron reduction of the α-bromocarbonyl by the α-amino radical as a propagation step cannot be excluded.
25. DFT calculations were performed with the use of B3LYP/6-311+G(2d,2p)//B3LYP/6-31G(d).
26. A conformer that positions the enamine olefin toward the *tert*-butyl group was also found to be energetically relevant in these calculations. Because of the pseudo C_2-symmetric nature of catalyst **6**, this enamine conformer also exists with the *Si* face open and the *Re* face blocked in a manner similar to DFT–**8**.
27. Materials and methods are available as supporting material on *Science* Online.
28. No rate enhancement was observed in the absence of $Ru(bpy)_3^{2+}$ with additive bpy or Bu_4NCl.
29. S. Oishi, N. Furuta, *Chem. Lett.* **7**, 45 (1978).
30. None of the remaining reaction components (aldehyde, amine catalyst, 2,6-lutidine, or 2,6-lutidinium bromide) quenched $*Ru(bpy)_3^{2+}$.

31. We thank S. Bernhard for his assistance in performing quenching experiments, as well as many insightful discussions. Additionally, we thank T. J. Rainey for performing DFT calculations. Financial support was provided by the NIH General Medical Sciences (grant R01 GM078201-01-01) and gifts from Merck, Amgen, and Bristol-Myers Squibb. D.A.N. is grateful for a NIH National Service Research Award fellowship (F32GM076816).

Supporting Online Material

www.sciencemag.org/cgi/content/full/1161976/DC1
Materials and Methods
Figs. S1 to S3
References

18 June 2008; accepted 8 August 2008
Published online 4 September 2008;
10.1126/science.1161976
Include this information when citing this paper.

Temperature-Induced Hydrophobic-Hydrophilic Transition Observed by Water Adsorption

Hai-Jing Wang, Xue-Kui Xi, Alfred Kleinhammes, Yue Wu*

The properties of nanoconfined and interfacial water in the proximity of hydrophobic surfaces play a pivotal role in a variety of important phenomena such as protein folding. Water inside single-walled carbon nanotubes (SWNTs) can provide an ideal system for investigating such nanoconfined interfacial water on hydrophobic surfaces, provided that the nanotubes can be opened without introducing excess defects. Here, we report a hydrophobic-hydrophilic transition upon cooling from 22°C to 8°C via the observation of water adsorption isotherms in SWNTs measured by nuclear magnetic resonance. A considerable slowdown in molecular reorientation of such adsorbed water was also detected. The observed transition demonstrates that the structure of interfacial water could depend sensitively on temperature, which could lead to intriguing temperature dependences involving interfacial water on hydrophobic surfaces.

Water in the immediate vicinity of hydrophobic surfaces plays a crucial role in various important phenomena such as the folding and activity of proteins (*1*, *2*), but experimental signatures of these water layers have proven difficult to obtain. One possibility is that the structures and dynamics of nanoconfined interfacial water could possess distinctive temperature dependences (analogous perhaps to the anomalous density maximum manifested by bulk water at 4°C). A temperature dependence in the properties of interfacial water could be important for various processes, such as the cold denaturation of proteins (*2*).

Single-walled carbon nanotubes (SWNTs) provide a model system for investigating the properties of nanoconfined interfacial water (*3*–*9*). Because each nanotube with diameter of 1.4 nm can only accommodate one layer of water molecules on their inside surface (*5*), the behavior of adsorbed water inside such SWNTs could provide important insight into the properties of nanoconfined interfacial water. A previous theoretical study showed that water could fill the interior of carbon nanotubes through favorable structural effects on the local excess chemical potential (*3*). This result implies that water could be adsorbed inside SWNTs below saturated vapor pressure, as demonstrated by previous studies (*10*, *11*). However, in those studies, the defect density and principal adsorption sites (PAS), known to alter water adsorption isotherms in activated carbon (*12*), were likely too high to reveal the intrinsic adsorption properties of SWNTs. Water

Department of Physics and Astronomy, University of North Carolina, Chapel Hill, NC 27599–3255, USA.

*To whom correspondence should be addressed. E-mail: yuewu@physics.unc.edu